

Received October 7, 2019, accepted October 15, 2019, date of publication October 29, 2019, date of current version November 13, 2019.

Digital Object Identifier 10.1109/ACCESS.2019.2950368

Speed Control of Load Torque Feedforward Compensation Based on Linear Active Disturbance Rejection for Five-Phase PMSM

ZHI KUANG¹, BOCHAO DU¹, SHUMEI CUI¹, AND C. C. CHAN, (Fellow, IEEE)

Department of Electrical Engineering, Harbin Institute of Technology, Harbin 150001, China

Corresponding author: Shumei Cui (cuism@hit.edu.cn)

This work was supported in part by the National Natural Science Foundation of China under Grant 51577035.

ABSTRACT This study focuses on the speed control problem of a five-phase permanent magnet synchronous motor (PMSM) in the presence of a variable load torque and unknown model parameters. To overcome the mutual transmission of motor torque ripple and load disturbance when the five-phase PMSM directly drives the load, a control method of load torque feedforward compensation based on linear auto disturbance rejection controller (LADRC) is proposed. First, the load torque observer is introduced to observe the load torque which is used as feedforward compensation to eliminate the effects of load torque changes. Second, an LADRC in the outer speed loop is presented to estimate the disturbance, and the stability of LADRC is analyzed. Third, the proposed torque feedforward method based on the LADRC is compared with the traditional proportional integral (PI) torque feedforward method. The PI regulators for current loops are designed. Finally, the simulation models are built and the control algorithms are both implemented using a TMS320F28335 DSP. The simulation and experiment results show that the proposed load torque feedforward compensation based on the LADRC produces excellent dynamic performance, such as smaller overshoot and faster response time. The proposed control scheme is robust and has a strong anti-disturbance ability, even in the case of large load torque disturbances.

INDEX TERMS Five phase PMSM, linear active disturbance rejection controller (LADRC), linear extended state observe (LESO), load torque observer.

I. INTRODUCTION

Owing to its fault-tolerant capability, high power density and high reliability, multiphase permanent magnet synchronous motor (PMSM) for variable speed applications have attracted considerable attention in various fields [1]. Five-phase PMSMs can directly drive loads without a reduction gear, which can make a drive system simple. However, two disturbance torques between motor torque ripple and load are directly transmitted to each other. In addition, the control system for multiphase PMSM is nonlinear with strong coupling and multivariable conditions leading to poor speed characteristics. When the system includes both internal and external disturbances, it struggles to cope with the

contradiction between rapidity and overshoot in a wide speed range using proportional integral (PI) regulators, so it is of importance to find a way to resist the unpredictable disturbance as much as possible.

The active disturbance rejection controller (ADRC) is a nonlinear control method proposed by Han in 1998 [2], and its working principle is to regard the unknown dynamics as the extended state of the controlled object, and then estimate it through extended state observer (ESO) and compensate its unknown dynamics in real time. ADRC resists disturbances from the outside and inside by estimating the speed loop and flux linkage of the induction motor [3]. To further overcome the uncertainty of disturbances estimation error and control gain, the sliding mode control method based on ADRC is proposed [4], [5], and the model prediction based on ADRC is used to accurately estimate the model

The associate editor coordinating the review of this manuscript and approving it for publication was Giambattista Gruosso¹.

parameters [6], [7]. A second-order ADRC-based speed controller is applied to induction motors powered by matrix converters [8]. To simplify the motor control system, three first-order ADRC are presented for the speed control of induction motor drives [9]. In addition, many researchers also have made their efforts to improve the performance of PMSM system based on ADRC. The question is also mainly focused on the speed control or precision position location. ADRC is used for direct torque control of permanent magnet synchronous servo motor [10], which can meet high speed regulation system requirements. The precise motion control of PMSM based on ADRC provides a simple way to implement the nonlinear friction compensation without any model [11]. Speed control of sensorless interior PMSM [12], [13] and position sensorless vector control of PMSM [14]–[16] based on ADRC are proposed, the disturbance for control system is observed and the speed was estimated. In the speed loop controller, the ADRC takes the external load disturbance and the internal model disturbances as the unknown disturbance of the system. In the current loop controller, the product term containing the speed is taken as the model uncertainty part, and the observation and compensation are respectively performed.

However, ADRC mentioned above is generally second-order or higher, and the design process is very complicated, especially when applying the algorithm. A large number of parameters need to be adjusted, and the operation time is long, which makes it difficult to use in practice. In this paper, the first-order linear active disturbance rejection controller (LADRC) controller is proposed to realize the speed closed-loop control of the five-phase PMSM system. This not only provides the ADRC’s anti-interference ability, but also simplifies the design of the control system. In engineering practice, actuator saturation is unavoidable, and, if not fully considered, it may cause serious performance degradation or even instability, especially in the control system. All disturbances are only estimated by extended state observer (ESO), greatly increasing the burden on the ESO. A load torque observer feedforward compensation is introduced to weaken the effects of load torque changes and alleviate the linear extended state observer (LESO) pressure of the LADRC.

In this paper, the LADRC in conjunction with the load torque observer is proposed to realize the speed control of the five-phase PMSM based on a space vector pulse width modulation (SVPWM) system. The stability of the LADRC for the speed loop is analyzed by the Jury criterion. The LADRC in outer speed loop combines the simplicity of a linear controller and the merit of the ADRC, which reduces the real running time of an algorithm on DSP and is not relying on a precise mathematical model. The load torque observer feedforward compensation in the inner loop is introduced to weaken the effects of load torque changes. The order of LADRC for a speed loop is low, making it very important to make the system simple and guarantee the stability of this proposed composite system.

II. THE LOAD TORQUE OBSERVER

The motor motion equation for the five-phase PMSM is given in the regulations positive direction of each physical quantity. The frictions, including static friction and coulomb friction are ignored to simplify the motion equation of the electric machine. The viscous friction for motor is considered as the part of motor motion equation, and the vector control of the five-phase surface-mount PMSM is controlled by the direct-axis current $i_d = 0$. The equations of motion and electromagnetism are expressed as follows [16], [17].

$$\frac{d\omega_m}{dt} = \frac{1}{J}(T_e - T_L - B_m\omega_m) \tag{1}$$

$$T_e = \frac{5}{2}n_p\psi_r i_q \tag{2}$$

where ω_m is the mechanical angular velocity of rotor, n_p is the number of polar pairs, J is the system moment of inertia, T_e is the electromagnetic torque of motor, T_L is load torque, B_m is the coefficient of viscous friction, ψ_r is the flux of main pole, and i_q is the quadrature component of the stator current.

The variation of load torque in one sampling period is considered to change very slowly compared with the rotor speed and position, therefore it is possible to assume that the variation of load torque is nearly zero [18].

$$\frac{dT_L}{dt} = 0 \tag{3}$$

Based on (1) and (3), the system model is expressed with the following state space equations:

$$\begin{cases} \frac{dx}{dt} = Ax + Bu \\ y = Cx \end{cases} \tag{4}$$

where x , A , u and B , C are given by

$$x = \begin{bmatrix} \omega_m \\ T_L \end{bmatrix}; \quad A = \begin{bmatrix} -B_m/J & -1/J \\ 0 & 0 \end{bmatrix};$$

$$B = \begin{bmatrix} 1/J \\ 0 \end{bmatrix}; \quad C = [1 \quad 0];$$

and $u = T_e$; $y = \omega_m$.

The actual output electromagnetic torque T_e is still taken as the input variable. The mechanical angular velocity $\hat{\omega}_m$ and the load torque \hat{T}_L are used as the state variables, and the output variable is the mechanical angular velocity. A simple linear state observer can be designed by using the standard control theory [18][19].

$$\begin{bmatrix} \dot{\hat{\omega}}_m \\ \dot{\hat{T}}_L \end{bmatrix} = \begin{bmatrix} -B_m/J & -1/J \\ 0 & 0 \end{bmatrix} \begin{bmatrix} \hat{\omega}_m \\ \hat{T}_L \end{bmatrix} + \begin{bmatrix} 1/J \\ 0 \end{bmatrix} T_e + L \left(\omega_m - [1 \ 0] \begin{bmatrix} \hat{\omega}_m \\ \hat{T}_L \end{bmatrix} \right) \tag{5}$$

where $\hat{x} = [\hat{\omega}_m \ \hat{T}_L]^T$ is an estimated state variables matrix and $L = [l_1 \ l_2]^T$ is the observer gain matrix for state feedback.

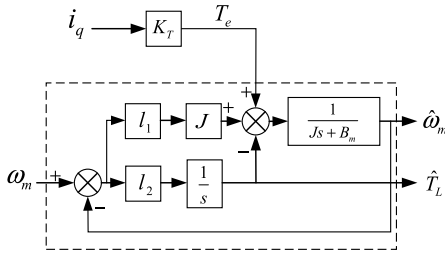


FIGURE 1. Schematic of load torque observer.

Subtracting (5) from the observer in (4), the error equation of the torque observer system can be obtained as follows:

$$\frac{d\bar{x}}{dt} = [A - LC]\bar{x} = \begin{bmatrix} -B_m/J - l_1 & -1/J \\ -l_2 & 0 \end{bmatrix} \begin{bmatrix} \omega_m - \hat{\omega}_m \\ T_L - \hat{T}_L \end{bmatrix} \quad (6)$$

where the observation error variable is defined by $\bar{x} = x - \hat{x}$.

The characteristic equation of (6) is given in (7), and the observer gain is determined using the pole placement method:

$$\det[sI - (A - LC)] = s^2 + (l_1 + B_m/J)s - l_2/J = 0 \quad (7)$$

If L is chosen to ensure that the $A-LC$ has a stable and appropriate eigenvalue, then \bar{x} will decay to zero. Regardless of the value of $\hat{x}(0)$, $\hat{x}(t)$ will converge to $x(t)$. Suppose that the design specifications for this system require that the two roots of the characteristic equation be placed at $s_1 = \alpha$ and $s_2 = \beta$, the expected characteristic polynomial is

$$(s - s_1)(s - s_2) = s^2 - (\alpha + \beta)s + \alpha\beta = 0 \quad (8)$$

The gains l_1 and l_2 are chosen to meet so that the coefficients of (7) are equal to those of (8), suppose that $B_m \approx 0$,

$$\begin{cases} l_1 = -(\alpha + \beta) \\ l_2 = -J\alpha\beta \end{cases} \quad (9)$$

The discrete equations for expanding equation (5) are as follows:

$$\begin{cases} \hat{\omega}_m(k+1) = \hat{\omega}_m(k) + h[-(B_m/J)\hat{\omega}_m(k) \\ -\hat{T}_L(k)/J + T_e/J + l_1(\omega_m - \hat{\omega}_m(k))] \\ \hat{T}_L(k+1) = \hat{T}_L(k) + h[l_2(\omega_m - \hat{\omega}_m(k))] \end{cases} \quad (10)$$

where ω_m is the current mechanical angular velocity of rotor, $\hat{\omega}_m(k)$ is the observed mechanical angular velocity of rotor in the previous state, $\hat{\omega}_m(k+1)$ is the current estimated mechanical angular velocity of rotor. $\hat{T}_L(k)$ is the estimated load torque in the previous state, $\hat{T}_L(k+1)$ is the current estimated load torque, h is the sampling step size.

According to (5), the load torque observer is designed, this structure of the load torque observer is simple and easy to realize. The schematic of the load torque observer is shown in Fig 1. K_T is the motor torque constant.

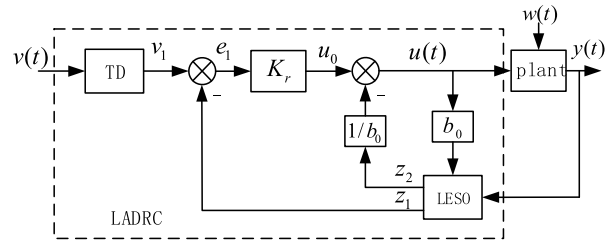


FIGURE 2. Block diagram of LADRC.

III. DESIGN LADRC FOR THE SPEED LOOP OF FIVE PHASE PMSM

Based on (1) and (2), the viscous torque and load torque are considered as two external disturbances for the speed closed loop. The moment of inertia for a rotor can be seen as one internal disturbance for the speed closed loop. The mathematical model of the speed control loop is

$$\frac{d\omega_m}{dt} = -(T_L - B_m\omega_m)/J + \frac{5n_p\psi_r}{2J}i_q \quad (11)$$

As is shown in Fig. 2, the LADRC consists of three parts: 1) tracking differentiator (TD), 2) LESO, and 3) linear state error feedback (K_r). The LESO in the LADRC feedback path provides the estimation of the unmeasured state. The structure of LESO is independent of the system model.

A. TD DESIGN

In a motor control system, the differential signal will unavoidably contain a certain amount of stochastic noise. TD can resolve the problem of differential signal extraction via integration. The linear track differential is built as follows.

$$\begin{cases} v_1(k+1) = v_1(k) + hv_2(k) \\ v_2(k+1) = v_2(k) + h(-r^2(v_1(k) - v(k)) - 2rv_2(k)) \end{cases} \quad (12)$$

where h is the sampling step, k denotes the k th sampling instant, r is speed factor, v_1 is the track signal of v , v_2 is differential signal of v .

B. LESO DESIGN AND STABILITY ANALYSIS

In LADRC, LESO is used to observe the state variables and estimate the total uncertainty as an extended state, which consists of internal dynamics and external disturbances. Equation (11) can be written as follows.

$$\begin{cases} \dot{x}(t) = w(t) + b_0u(t) \\ y = x(t) \end{cases} \quad (13)$$

where, $w(t) = -(T_L - B_m\omega_m)/J$, the total disturbance $w(t)$ is in a bounded domain, the coefficient of control variable $u(t)$ is known, $b_0 = 5n_p\psi_r/2J$, the control variable $u(t)$ is the output of the speed loop and is used to adjust the quadrature component of the motor stator current.

The discrete algorithm of LESO can be defined as follows.

$$\begin{cases} e(k) = z_1(k) - y(k) \\ z_1(k+1) = z_1(k) + h(z_2(k) - \beta_{01}e(k) + b_0u(t)) \\ z_2(k+1) = z_2(k) - h\beta_{02}e(k) \end{cases} \quad (14)$$

where β_{01} and β_{02} are the parameters to be adjusted and $y(k)$ is the output of the controlled plant. LESO can not only obtain the estimated output of $z_1(k)$ but it can also estimate the total disturbance $z_2(k)$. The disturbance in the system, caused by nonlinear dynamics, model uncertainty and external factors, can be observed in real-time and compensated for by LESO.

Let $e(k) = z_1(k) - x(k)$, $\eta(k) = z_2(k) - w(k)$. Subtracting the discretized (13) from (14), the error function is as follows

$$\begin{bmatrix} e(k+1) \\ \eta(k+1) \end{bmatrix} = \begin{bmatrix} 1 - \beta_{01}h & h \\ -h\beta_{02} & 1 \end{bmatrix} \begin{bmatrix} e(k) \\ \eta(k) \end{bmatrix} - \begin{bmatrix} 0 \\ w(k+1) - w(k) \end{bmatrix} \quad (15)$$

According to (3), $w(k+1) - w(k)$ is a high-order infinitesimal function of step h , which is negligible, and the equation is expressed as follows.

$$\begin{bmatrix} e(k+1) \\ \eta(k+1) \end{bmatrix} = A \begin{bmatrix} e(k) \\ \eta(k) \end{bmatrix} \quad (16)$$

where $A = \begin{bmatrix} 1 - \beta_{01}h & h \\ -h\beta_{02} & 1 \end{bmatrix}$, then the characteristic equation of A is as follows.

$$A(z) = \det(zI - A) = z^2 + (\beta_{01}h - 2)z + 1 - \beta_{01}h + \beta_{02}h^2 \quad (17)$$

According to the Jury criterion, to stabilize the LESO of the speed loop, the characteristic root of $A(z)$ must be within the unit circle, the stability conditions of the LESO are as follows.

$$\begin{cases} |1 - \beta_{01}h + \beta_{02}h^2| < 1 \\ |2 - \beta_{01}h| < 2 - h\beta_{01} + \beta_{02}h^2 \end{cases} \quad (18)$$

Therefore, the LESO parameters of the speed loop can be set according to the following principles [12].

$$\beta_{01}h = 1, \quad \beta_{02}h^2 = 0.3 \quad (19)$$

C. K_r DESIGN

The LADRC uses K_r to improve the performance of the controller which makes the implementation time of an algorithm on DSP short and simple. $u_0(k)$ is used to drive the state trajectory to the desired reference signal. Its mathematic expression in Fig. 2 is given as

$$\begin{cases} u_0(k) = K_r(v_1(k) - z_1(k)) \\ u(k) = u_0(k) - z_2(k)/b_0 \end{cases} \quad (20)$$

When $z_2(k)$ can accurately estimate the total of disturbance $w(t)$, this control object can be converted to an integrator series-type. It is obvious that LADRC is independent of the plant model. With the help of the estimated value of the disturbance and uncertain term, the compensation is made. Hence, LADRC has good adaptability and robustness for plant in a certain range.

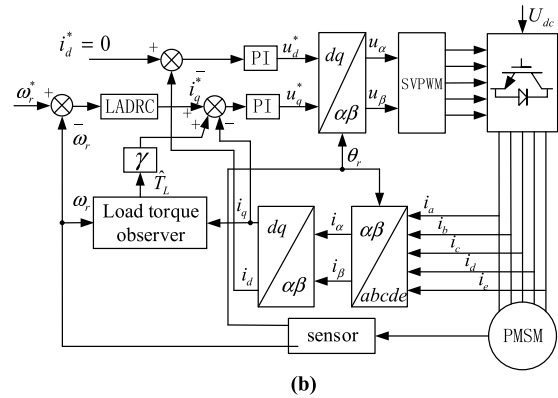
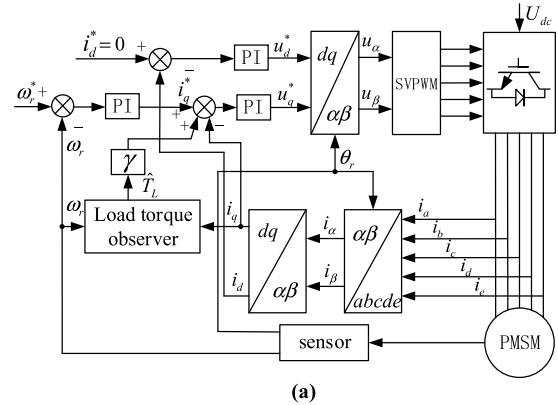


FIGURE 3. Two different speed control systems (a) based on PI regulation and load torque feedforward (b) combined LADRC and load torque feedforward.

IV. THE MODEL OF TORQUE FEEDFORWARD COMPENSATION BASED ON LADRC

For the surface mounted five-phase PMSM, the inductances between the d-axis and q-axis are equal in the theory. The given direct component of stator current $i_d^* = 0$. After the coordinate transformation, the dynamic model of the five-phase PMSM under the rotor coordinate reference is expressed as follows.

$$u_d = r i_d + L_d \frac{di_d}{dt} - L_q i_q \omega_e \quad (21)$$

$$u_q = r i_q + L_q \frac{di_q}{dt} + \omega_e L_d i_d + \omega_e \psi_r \quad (22)$$

where ω_e is the electrical angular velocity of rotor and r is armature resistance of stator windings per phase.

During load torque disturbance, there are usually corresponding speed fluctuations, which are determined by the inherent characters of PI regulators. To eliminate the influence of the load disturbance on the rotational speed system, the load torque feedforward is used to compensate for the disturbance change. A speed control system based on PI regulation and load torque feedforward is shown in Fig. 3 (a). To verify the validity of the proposed combined LADRC and load torque feedforward, the control model of LADRC and the load torque feedforward compensation for five-phase PMSM are shown in Fig. 3 (b).

TABLE 1. Parameters for LADRC and current closed-loop.

Parameters	Value
Simulation step h	1e-4
LESO gain β_{01}	1e4
LESO gain β_{02}	3e7
Linear state error feedback K_r	12
Proportional gains of the current regulators K_{pi}	5
Integral gains of the current regulators K_{ii}	24

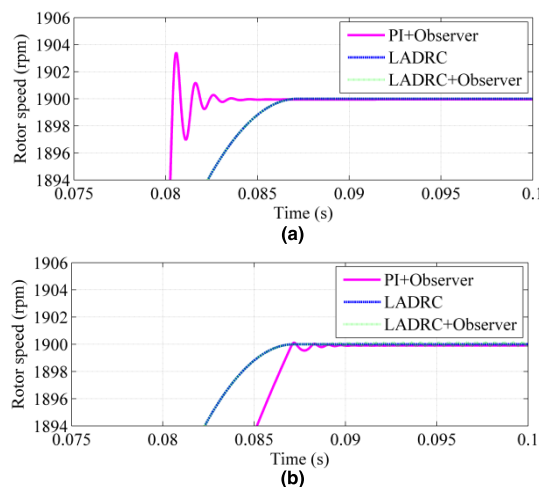
In Fig. 3 (a), there are three PI regulators: one for speed loop regulation and the other two for decoupled quadrature axis current and direct axis current regulation. The difference is that the LADRC replaces the PI regulator in the speed loop in Fig. 3 (b). Both of the torque feedforwards are used to eliminate the influence of the torque change on the speed control. The compensation factor of the load torque is γ . The motivation for using the LADRC is to reduce the complexity of the control algorithm and increase the robustness of speed control system when it is implemented on DSP. The LADRC design method has been described in Section III and consists of three parts. The LESO in the LADRC feedback path provides the estimation of the unmeasured state. The structure of LESO is independent of the system model. Its performance is determined by the range of its variation rate, and this is the main reason that LADRC is robust and adaptive. These factors give the LADRC a reasonable balance between the fast transient response, and small overshoot. On the contrary, the conventional PI controller struggles to achieve this point by tuning parameters because the fast response and small overshoot are contradictory for the PI controller.

V. SIMULATION RESULTS

In this paper, a 20-pole 10kw five-phase PMSM is designed as a research model. A computer simulation is conducted to evaluate the proposed combination of the LADRC and load torque observer by using the five-phase PMSM. A MATLAB/Simulink model has been established. The parameters of the five-phase PMSM are listed as follows $P_N = 10$ kW, $U_N = 120$ V, $I_N = 25$ A, $L_d = 1.6$ mH, $L_q = 1.6$ mH, $R_s = 0.26$ Ω , $n_p = 10$, $T_L = 45$ Nm, $J = 0.01$ kg·m², $n_N = 1900$ rpm, $\psi_r = 0.056$ Wb.

The simulation results based on SVPWM for the five phase PMSM driven by a voltage source inverter are compared between the proposed control scheme and traditional PI torque feedforward compensation under the same conditions. In addition, the simulation results between the proposed method and LADRC without load torque observer are compared. Both parameters of the LADRC and those of PI regulators have been manually tuned to their optimal values. The parameters for LADRC and speed loop are shown in TABLE 1.

The five-phase PMSM speed response curves of the three simulation models are compared, including the PI regulator plus torque feedforward compensation of the torque observer (PI + Observer), the LADRC without torque feedforward

**FIGURE 4.** Comparative dynamic response result of speed regulation under different load conditions. (a) no load (b) rated load.

compensation, and the LADRC plus the torque feedforward compensation of the torque observer (LADRC + Observer). Three cases are considered to demonstrate the validity of the proposed method: 1) speed response; 2) load disturbance; 3) the motor parameter variations.

A. SPEED RESPONSE

Fig.4 (a) shows the speed response from zero to the rated speed under no load conditions. Under rated load conditions, those of the speed response are shown in Fig. 4 (b).

When the traditional PI torque feedforward compensation system starts from zero to rated speed under no-load conditions, the speed overshoot is 0.16%. When the system starts from zero to rated speed under rated load conditions, the overshoot is almost zero. However, the settling time of the rated load start is longer than the settling time of the no-load start. The speed response of five-phase PMSM system between LADRC and the proposed method shows nearly no overshoot and is comparatively stable in both conditions. The response time to a stable-state is short, and speed can be traced without any stable-state error. When the rotor speed is close to reference speed under rated load conditions, the speed of PI regulators and feedforward compensation fluctuates a little and it needs time to settle down to a stable-state with some stable-state error.

B. LOAD DISTURBANCE PERFORMANCE

Fig. 5 shows the dynamic response of the proposed control method, the traditional PI torque feedforward compensation, and the LADRC without torque feedforward compensation. Fig. 5 (a) shows the corresponding speed curve at rated speed 1900rpm, rated load torque applied to the five-phase PMSM at 2 s, and sudden change from rated load torque to no load at 2.2 s. In order to verify the performance of the proposed control method over a wide speed range, the same parameters for the LADRC, current loop PI regulators, and torque observer are applied to the five-phase PMSM at low speeds,

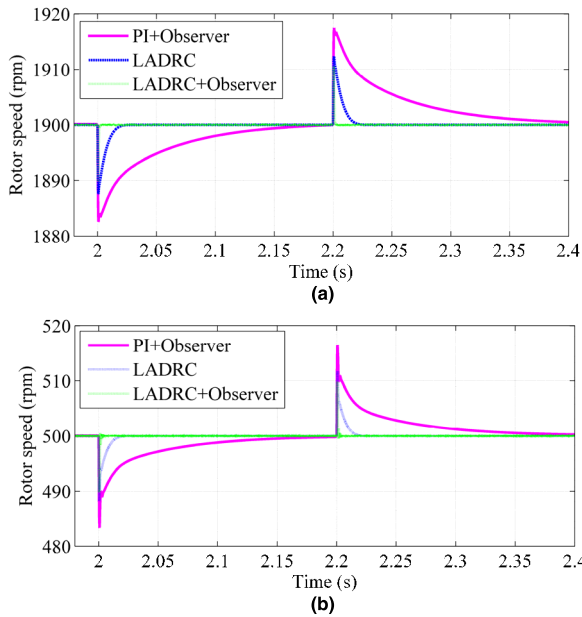


FIGURE 5. Dynamic response of different control schemes during step load changes at different rotational speed (a) 1900rpm (b) 500rpm.

TABLE 2. Rotational speed fluctuation error when the load changes.

Control methods	Fluctuation error			
	Load step down		Load step up	
	500rpm	1900rpm	500rpm	1900rpm
PI + Observer	3.6%	0.94%	3.4%	0.94%
LADRC	2.4%	0.63%	2.2%	0.62%
LADRC + Observer	2%	0.52%	2%	0.57%

where a low speed is defined as 500 rpm. Fig. 5 (b) shows the speed response curve when rated load torque steps up at 2s and steps down at 2.2 s under the low speed conditions.

Regardless of whether the rotational speed of the five-phase PMSM is at 1900 rpm or 500 rpm, the rotational speeds of the three control methods fluctuate when the load changes. The rotational speed fluctuation error is shown in TABLE 2. It can be seen from TABLE 2 that regardless of the five-phase PMSM rotor speed, the proposed control method has a rotational speed fluctuation error less than the LADRC when the load is suddenly increased or decreased, and the LADRC rotational speed fluctuation error is smaller than traditional PI torque feedforward compensation. In summary, the proposed control method speed fluctuation is the smallest of the three control methods.

As shown in Fig. 5, the speed response of the proposed method is faster than that of the PI regulator feedforward compensation when the load sudden change. The phenomenon is because LADRC system is more robust than the PI regulator feedforward compensation, when considering load disturbance. The reason is that when torque control and flux are decoupled completely using field-oriented control,

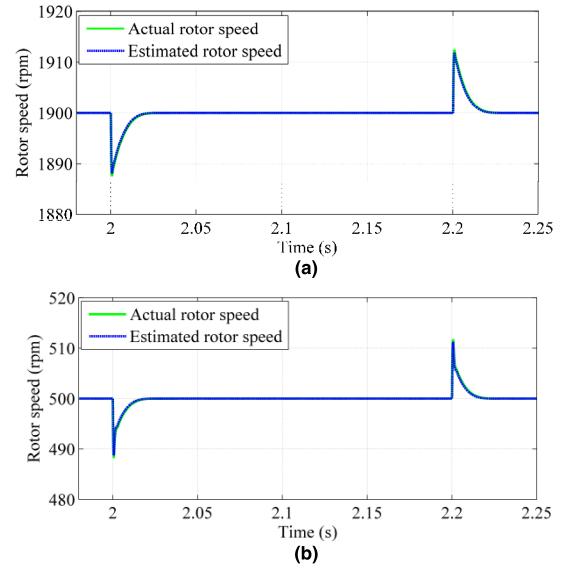


FIGURE 6. Comparative actual and estimated rotor speed under different rotational speed conditions. (a) 1900 rpm (b) 500 rpm.

the five-phase PMSM is treated as a linear system for PI regulators, while the LADRC estimates the total disturbances including internal and external disturbances and compensates for them, so that the system is dynamically linearized. When load torque changes, the LESOs of LADRCs can precisely estimate the disturbance in form of (13), and quickly output the corresponding adjustment value. However, PI regulators and feedforward compensation still linearly regulate the adjustment value to cope with the variation in load torque. In addition, the torque feedforward compensation of the torque observation further resists the disturbance caused by the torque fluctuation. Therefore, the combined control method of LADRC and load torque observer can maintain its good dynamic performance, such as fast response of speed, no overshoot and good ability to resist disturbance, under different operation conditions. The proposed method is suitable for different operational conditions without the need for parameter changes.

Fig. 6 show the actual and estimated rotor speed for the LADRC under two different rotor speeds, that the load torque steps up from no load to rated load at 2 s, and from the rated load to no load at 2.2 s. The simulation results show that there is no difference between the actual rotational speed and the values estimated by the LESO. These figures indicate that the LESO can successfully track the state variables of the five-phase PMSM.

When the load is suddenly increased or decreased, the motor load torque observed by the torque observer is as shown in Fig. 7. The observed torque almost completely follows the given load torque. Only when the five-phase PMSM load torque is accurately estimated, can the torque feedforward compensation be performed according to the motor load torque. To balance the stability of the system, the torque feedback coefficient needs to be an

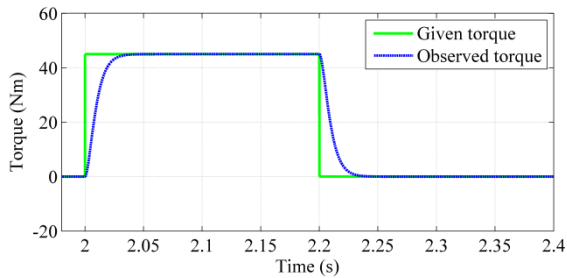


FIGURE 7. Observed load torque under rotational speed 1900rpm.

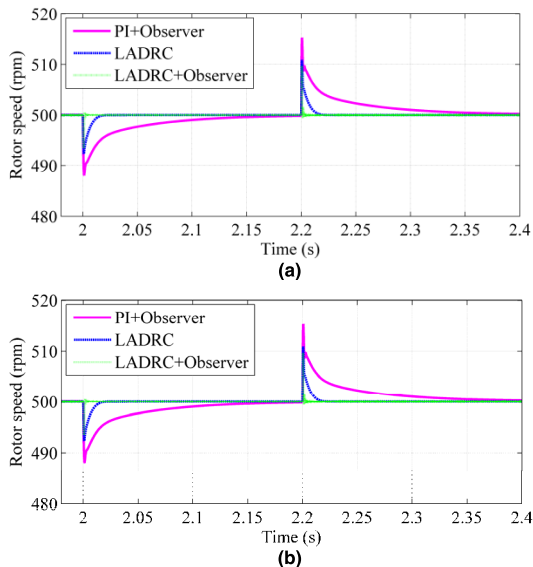


FIGURE 8. Speed response curve when the magnetic flux of the permanent magnet changes under different speed conditions. (a) 1900 rpm. (b) 500 rpm.

appropriate value. In this simulation system, $\gamma = 0.4$, and $\alpha = \beta = -200$.

C. PARAMETER VARIATIONS PERFORMANCE

As mentioned before, the variation of motor parameters will influence the performance of the control system. The simulation induction motor model for a varying rotor resistance has been built [20], but rotor of the five-phase PMSM has no windings. The rapid parameter variation is not the general case, because the resistance of stator changes slowly with the temperature rise in the operation motor. To inspect the influence of the motor system under parameter variations, the flux of the permanent magnet is chosen to generate step changes in the simulation model at rated torque and constant rotor speed. The magnetic flux of the permanent magnet is used as a standard unit (1pu) under rated load conditions, and the magnetic flux of the permanent magnet on the rotor steps down from 1pu to 0.5pu at 2s and step up from 0.5pu to 1pu at 2.2s. Fig. 8 shows the comparison of the rotational speed response curves when the magnetic flux of the permanent magnet changes under different rotational speed conditions.

TABLE 3. Rotor speed fluctuation error when the magnetic flux changes.

Control methods	Fluctuation error			
	Flux step down		Flux step up	
	500rpm	1900rpm	500rpm	1900rpm
PI + Observer	2.4%	0.64%	3.2%	0.69%
LADRC	1.6%	0.37%	2.4%	0.48%
LADRC + Observer	1.2%	0.26%	2%	0.42%

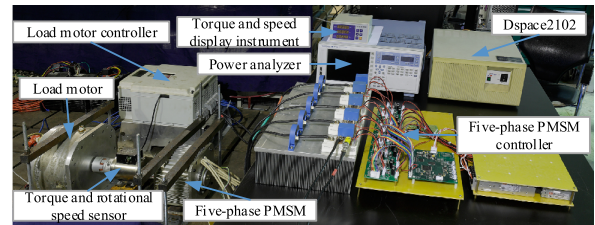


FIGURE 9. Photograph of the experimental bench.

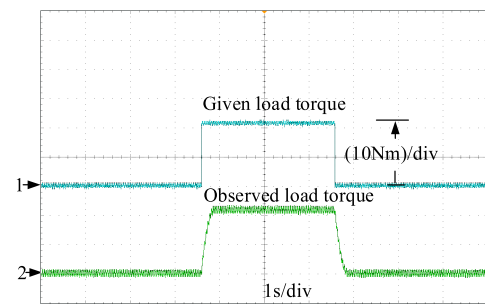


FIGURE 10. Waveform of the torque observer tracking load torque.

The rotational speeds of the three control methods fluctuate when the magnetic flux of the permanent magnet changes under different speed conditions. The rotational speed fluctuation error is shown in TABLE 3.

As shown in Fig. 8, at both 1900 rpm and 500 rpm, the proposed method can still maintain good speed regulation in spite of parameter changes. However, the PI regulators feedforward compensation system deteriorates significantly, and rotational speed fluctuates greatly during parameter changes. The reason is that the LADRC in speed loop resists the disturbance. Moreover, the torque feedforward compensation can also effectively resist the torque disturbance caused by the parameter changes. Therefore, the combined control method of the LADRC and load torque observer is able to quickly complete the adjustment process, and stabilize at the reference speed again. The proposed method is more robust than the PI regulators feedforward compensation.

VI. EXPERIMENTAL RESULTS

A workbench is built to validate performance of the proposed method for the five-phase PMSM seen in Fig. 9. The actual five-phase PMSM has the same controller parameters as those

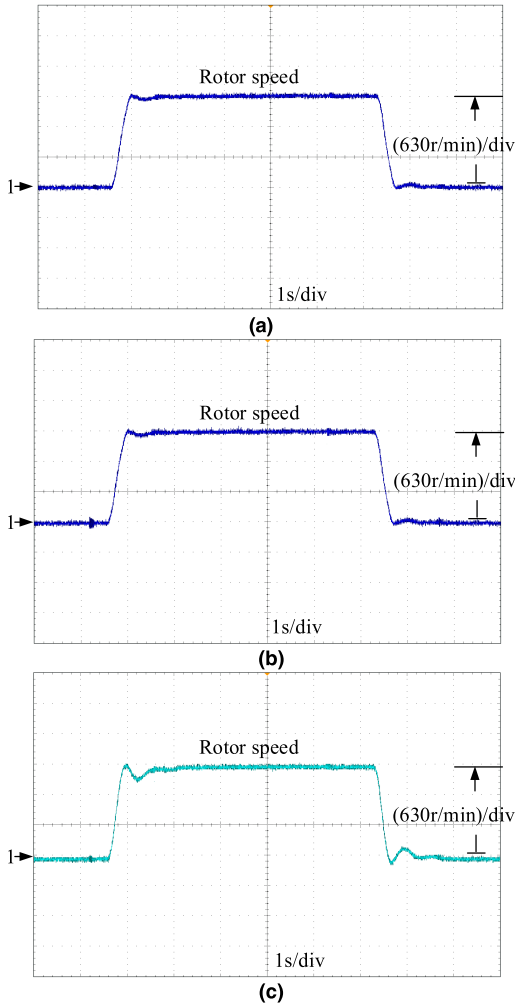


FIGURE 11. Startup performance for the five phase PMSM with no load under different control modes (a) LADRC + Observer (b) LADRC (c) PI + Observer.

used in the simulations. The comparative experiment between the LADRC and PI regulators are implemented on the same control circuit, in which the core is TMS320F28335 DSP. The switching frequency of the PWM signal is 10 kHz. The A/D board is designed with an AD7606. The load torque is supplied by a three-phase permanent magnet synchronous motor, which is controlled by DSPACE 2102. It is convenient to accurately control action time for the given load torque. The LADRC algorithm and torque observer are written in C mixed language. The differences between LADRC and traditional ADRC are the state error feedback, and the way of disturbance observation. The LADRC use the linear functions, while ADRC use the nonlinear functions which contains exponent functions, so the execution time of LADRC is shorter than ADRC. The algorithm of the LADRC is simple on TMS320F28335 DSP.

Fig. 10 shows the waveform of the torque observer tracking the load torque. The load torque observer accurately tracks changes in the given load torque at 500 rpm. The observed load torque value is divided by the motor torque coefficient into the q-axis current value, then multiplied by the torque

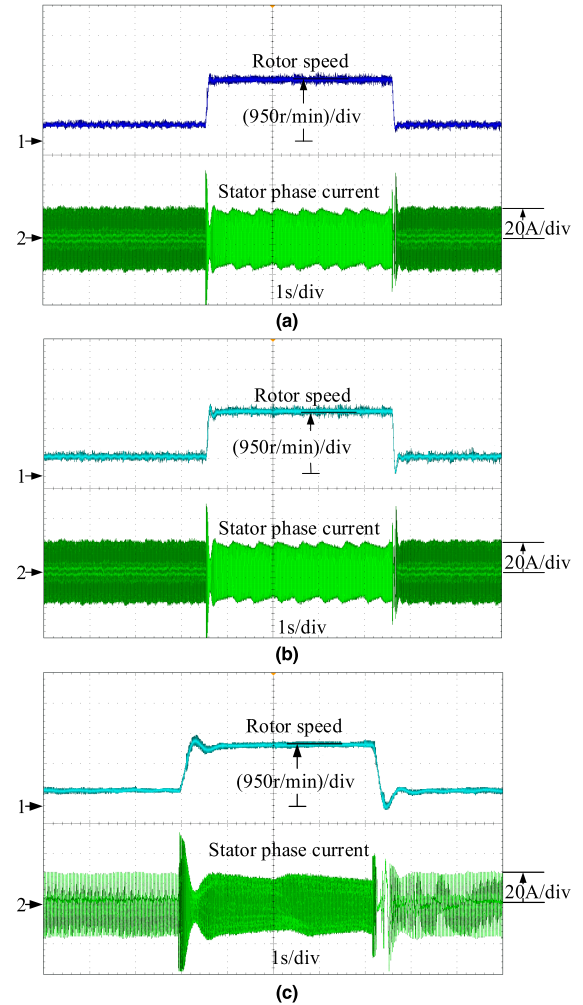


FIGURE 12. Comparative experimental results in different control modes for a given speed change at rated load torque (a) LADRC + Observer (b) LADRC (c) PI + Observer.

feedback coefficient for the current closed-loop torque feedforward compensation to suppress the disturbance effect of the load change. The accuracy of the observed load torque is a prerequisite for torque feedforward compensation.

Fig. 11 show the startup performance for the five-phase PMSM with no load. The speed response of the LADRC shows nearly no overshoot and is comparatively stable at 0.6s. The speed fluctuation of the PI torque feedforward compensation system is about 12% of the target speed, and the settle time is about 1s. The experimental results in Fig.11 are consistent with the simulation results in Fig. 4.

Fig. 12 shows the rotational speed response of the five-phase PMSM using the proposed method and the other two methods when the reference speed is changed at rated load torque. The rated load torque is measured as standard unitary (1pu). The given speed is set from 500 rpm to 1900 rpm, then returns from 1900 rpm to 500 rpm. The PI torque feedforward compensation speed response overshoot is about 10%. The speed response of the torque feedforward compensation based on the LADRC is better than that of the LADRC without torque feedforward compensation.

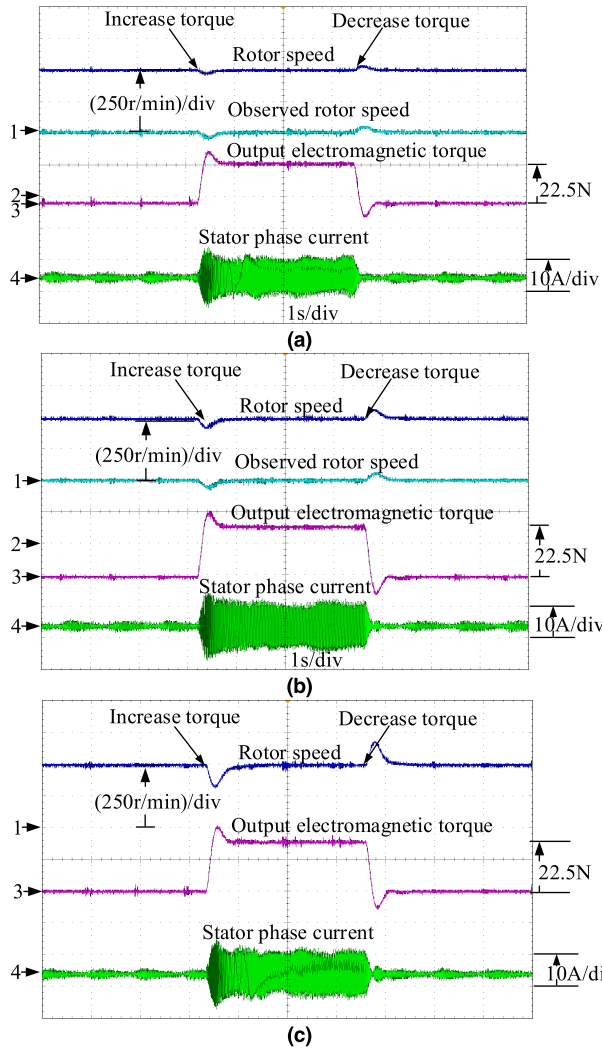


FIGURE 13. Comparative experimental results under different control modes when the load torque is abruptly changed at a reference speed of 500 rpm. (a) LADRC + Observer (b) LADRC (c) PI + Observer.

Fig. 13 show the comparative experimental results between the proposed load torque feedforward compensation based on LADRC and the other two methods when the load torque is suddenly changed under the set speed of 500 rpm. The speed response of the proposed method is better than that of the other two methods, and the experimental results are consistent with the simulation results in Fig. 5. The parameters between the motor and PI regulators in simulation are ideal, but it is hard to recreate these in practice. Fig. 14 show the comparative experimental results under the same conditions as in Fig. 13, except that the reference speed is 1900 rpm. The settle time of the PI regulators torque feedforward compensation is longer than that of the LADRC, and the speed variation is obvious during the transient state. It can be seen from simulated and experimental results that the proposed method with the LADRC is robust and adapts to external and internal disturbance. Their dynamic performances are better than that of the PI regulators torque feedforward compensation under parameter changes in a wide speed range.

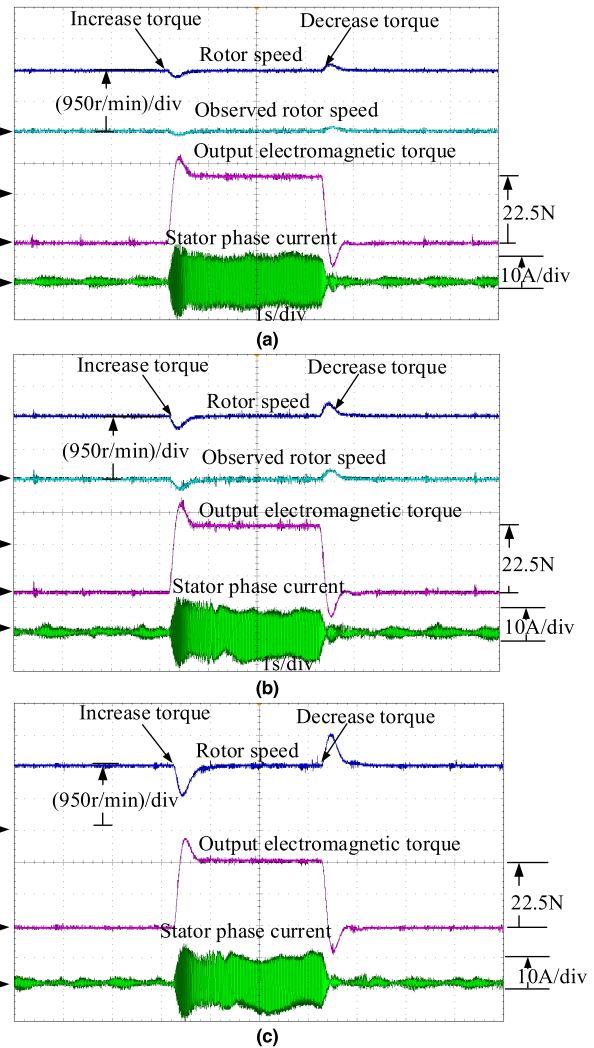


FIGURE 14. Comparative experimental results under different control modes when the load torque is abruptly changed at a reference speed of 1900 rpm. (a) LADRC + Observer (b) LADRC (c) PI + Observer.

Moreover, the torque feedforward compensation can also effectively resist the torque disturbance caused by the parameter changes.

VII. CONCLUSION

The torque feedforward compensation based on the LADRC successfully achieves the speed control of a five-phase PMSM driven by voltage source inverter. The LESO is the core component of the LADRC, and accurately estimates each variable and disturbance, including load disturbance and system parameter changes. The designed load torque observer can accurately track the change of load, and the load torque feedforward compensation can effectively suppress the disturbances caused by parameters such as load torque. The simulation results show that the proposed method achieves a good speed response under modeling parameter uncertainty and load disturbance. The experimental results show that the proposed method produces better dynamic performance, such as small overshoot and fast response, than the

PI regulators torque feedforward compensation when the disturbance occurs in its overall operational conditions. The LADRCs are independent of the detailed system model, so the proposed method is robust and adaptive.

REFERENCES

- [1] E. Levi, "Multiphase electric machines for variable-speed applications," *IEEE Trans. Ind. Electron.*, vol. 55, no. 5, pp. 1893–1909, May 2008.
- [2] J. Han, "Auto-disturbances-rejection controller and its applications," *Control Decis.*, vol. 1, pp. 19–23, Jan. 1998.
- [3] G. Feng, Y.-F. Liu, and L.-P. Huang, "A new robust algorithm to improve the dynamic performance on the speed control of induction motor drive," *IEEE Trans. Power Electron.*, vol. 19, no. 6, pp. 1614–1627, Nov. 2004.
- [4] F. Alonge, M. Cirrincione, F. D'Ippolito, M. Pucci, and A. Sferlazza, "Ippolito, M. Pucci, and A. Sferlazza, "Robust active disturbance rejection control of induction motor systems based on additional sliding-mode component," *IEEE Trans. Ind. Electron.*, vol. 64, no. 7, pp. 5608–5621, Jul. 2017.
- [5] C. Dai, J. Yang, Z. Wang, and S. Li, "Universal active disturbance rejection control for non-linear systems with multiple disturbances via a high-order sliding mode observer," *IET Control Theory Appl.*, vol. 11, no. 8, pp. 1194–1204, May 2017.
- [6] L. Yan, F. Wang, M. Dou, Z. Zhang, R. Kennel, and J. Rodriguez, "Active disturbance rejection-based speed control in model predictive control for induction machines," *IEEE Trans. Ind. Electron.*, to be published, doi: 10.1109/TIE.2019.2912785.
- [7] Z.-G. Liu and S.-H. Li, "Active disturbance rejection controller based on permanent magnetic synchronous motor model identification and compensation," *Proc. Chin. Soc. Elect. Eng.*, vol. 28, no. 24, pp. 118–123, Aug. 2008.
- [8] Y. Mei and L. Huang, "A second-order auto disturbance rejection controller for matrix converter fed induction motor drive," in *Proc. IEEE 6th Int. Power Electron. Motion Control Conf.*, May 2009, pp. 1964–1967.
- [9] J. Li, H.-P. Ren, and Y.-R. Zhong, "Robust speed control of induction motor drives using first-order auto-disturbance rejection controllers," *IEEE Trans. Ind. Appl.*, vol. 51, no. 1, pp. 712–720, Jan. 2015.
- [10] D. Liu, C. Che, and Z. Zhou, "Permanent magnet synchronous motor control system based on auto disturbances rejection controller," in *Proc. Int. Conf. Mechatronic Sci. Electr. Eng. Comput. (MEC)*, Aug. 2011, pp. 8–11.
- [11] Y. X. Su, C. H. Zheng, and B. Y. Duan, "Automatic disturbances rejection controller for precise motion control of permanent-magnet synchronous motors," *IEEE Trans. Ind. Electron.*, vol. 52, no. 3, pp. 814–823, Jun. 2005.
- [12] B. Du, S. Wu, S. Han, and S. Cui, "Application of linear active disturbance rejection controller for sensorless control of internal permanent-magnet synchronous motor," *IEEE Trans. Ind. Electron.*, vol. 63, no. 5, pp. 3019–3027, May 2016.
- [13] J. Wen and B. Cao, "Active disturbances rejection control speed control system for sensorless IPMSM," *Proc. CSEE*, vol. 29, no. 30, pp. 58–62, Oct. 2009.
- [14] G. Wang, R. Liu, N. Zhao, D. Ding, and D. Xu, "Enhanced linear adrc strategy for HF pulse voltage signal injection-based sensorless IPMSM drives," *IEEE Trans. Power Electron.*, vol. 34, no. 1, pp. 514–525, Jan. 2019.
- [15] G. Zhang, G. Wang, B. Yuan, R. Liu, and D. Xu, "Active disturbance rejection control strategy for signal injection-based sensorless IPMSM drives," *IEEE Trans. Transport. Electrific.*, vol. 4, no. 1, pp. 330–339, Mar. 2018.
- [16] K. Sun, Z. Xu, and J. Zou, "Novel approach to position sensorless vector control of PMSM based on active-disturbance rejection controller," *Proc. CSEE*, vol. 27, no. 3, pp. 18–22, Jan. 2007.
- [17] P. Pillay and R. Krishnan, "Modeling of permanent magnet motor drives," *IEEE Trans. Ind. Electron.*, vol. IE-35, no. 4, pp. 537–541, Nov. 1988.
- [18] K. B. Lee, J. Y. Yoo, J. H. Song, and I. Choy, "Improvement of low speed operation of electric machine with an inertia identification using ROELO," *IEE Proc.—Electric Power Appl.*, vol. 151, no. 1, pp. 116–120, Jan. 2004.
- [19] W. Lu, Y. Hu, J. Liang, and W. Huang, "Anti-disturbance adaptive control for permanent magnet synchronous motor servo system," *Proc. CSEE*, vol. 31, no. 3, pp. 75–81, Jan. 2011.
- [20] G. Feng, L. Huang, and D. Zhu, "A robust controller for improving disturbance rejection in speed control of induction motors," in *Proc. IEEE Int. Conf. Power Electron. Drive Syst.*, Jul. 1999, pp. 432–437.



ZHI KUANG was born in Hubei, China, in 1983. He received the B.S. degree from the Taiyuan University of Technology, Taiyuan, in 2006, and the master's degree from the Harbin Institute of Technology, Harbin, China, in 2009, where he is currently pursuing the Ph.D. degree with the Department of Electrical Engineering. His research interests include multiphase motor drive, fault tolerance operation, and power electronics.



BOCHAO DU was born in Heilongjiang, China, in 1986. He received the B.S., M.S., and Ph.D. degrees in electrical engineering from the Harbin Institute of Technology (HIT), Harbin, China, in 2009, 2011, and 2016, respectively. He is currently a Lecturer with HIT. His research interests include motor fault diagnosis and fault tolerance operation, motor parameter estimation, power electronics, and motor drivers.



SHUMEI CUI was born in Heilongjiang, China, in 1964. She received the Ph.D. degree in electrical engineering from the Harbin Institute of Technology (HIT), Harbin, China, in 1998.

She has been a Professor with the Department of Electrical Engineering, HIT. Her research interests include the design and control of micro and special electric machines, electric drive system of electric vehicles, control and simulation of hybrid electric vehicles, and intelligent test and fault diagnostics of electric machines. She serves as the Vice Director Member of the Micro and Special Electric Machine Committee and the Chinese Institute of Electronics, and a member of the Electric Vehicle Committee and the National Automotive Standardization Technical Committee.



C. C. CHAN (F'92) was born in 1937. His work is directly involved in the forefront of electric machines, electric drive, electric vehicles, and smart energy systems. He made great contributions in building up the fundamental theory of modern electric vehicles and exploring the correlation between Energy and Information. He proposed many insightful concepts most recently, including smart energy systems, energy computer, energy bank, and so forth. He was elected as an Academician of the Chinese Academy of Engineering and a Fellow of the Royal Academy of Engineering, U.K., in 1997.

...